SI Appendix

for

Motional dynamics of single Patched1 molecules in cilia are controlled by Hedgehog and cholesterol

Lucien E. Weiss[a,1], Ljiljana Milenkovic[b,1], Joshua Yoon[a,c], Tim Stearns[b,d], W. E. Moerner[a,2]

Departments of Chemistry[a], Biology[b], Applied Physics[c], and Genetics[d],

Stanford University

Stanford, CA, 94305, U.S.A.

[1]These authors contributed equally to this work.

[2]Corresponding author

Table of Contents

www.pnas.org/cgi/doi/10.1073/pnas.1816747116

A. Reagents, Cell lines, Labeling, Bulk Immunofluorescence

Small Molecules and Recombinant Proteins. Small molecules used in this study included: SAG (Enzo Life Sciences), SANT-1 (EMD Millipore), Methyl-β-cyclodextrin (MβCD, Sigma), Puromycin (Sigma), Polybrene (Millipore), DAPI (Invitrogen).
Human Sonic Hedgehog (SHH) carrying two isoleucine residues at the N-terminus and a hexahistidine tag at the C-terminus was expressed in *Escherichia coli* Rosetta(DE3)pLysS cells and purified by immobilized metal-affinity chromatography followed by gel-filtration chromatography as described previously by Bishop et al (1).
Domain 4 of bacterial toxin Perfringolysis O, tagged with EGFP (EGFP-D4H), has been previously described as a biosensor that can be used to visualize cholesterol in the plasma membrane (2). Purified, recombinant EGFP-D4H probe was a kind gift from Drs. Rajat Rohatgi and Giovanni Luchetti.

Antibodies. The primary antibodies used for immunostaining and immunoblot analysis were: mouse anti-acetylated Tubulin (Sigma), rabbit anti-SMO (3), rabbit anti-PTCH1 (3), rabbit anti-SNAP (NEB), mouse anti-Arl13b (Antibodies Incorporated), mouse anti-GFP (Invitrogen), rabbit anti-GFP (Abcam), mouse anti-gamma-Tubulin (Sigma). The secondary antibodies were from Invitrogen/Molecular probes and LI-COR Biosciences.

Constructs. The construct for mouse PTCH1 with a YFP-tag on its C-terminus in the MSCVpac vector was previously described (3). To make the plasmid encoding PTCH1-ACP-YFP in MSCVpac, the sequence for ACP tag, amplified by PCR from the pACP-tag(m)2 vector (NEB) was inserted into the unique AvrII restriction site of PTCH1-YFP by using In-fusion cloning kit (Clontech). The $5HT_6$-YFP expression vector was kindly provided by Dr. Takanari Inoue (4).

Transient Transfection and Retroviral Infection. Transient transfection of cells was done using Fugene-6 (Promega). All stable cell lines were made by infecting the cells with pMSCV-based retroviruses (Clontech), carrying the constructs of interest. Retroviral supernatants were produced in Bosc23 packaging cells and collected 48h after the transfection.

Cell culture. Cells were grown in high-glucose DMEM (Invitrogen), containing 10% Fetal Calf Serum (FCS, Hyclone). For all experiments, to promote ciliogenesis, cells were transferred to 0.5% FCS media for 24h.

Cell Lines. Previously described cell lines include: *ptch1-/-*, [*ptch1-/-; SNAP-Smo*], [*ptch1-/-; ptch1-YFP*] and [*smo-/-; SNAP-Smo*] MEF*s* (3, 5, 6). NIH 3T3 cells are from ATCC. Newly generated lines include: [*ptc1-/-;Ptch1-ACP-YFP]* cells generated by infection of *ptch1-/-* cells with a retrovirus carrying *Ptch1-ACP-YFP*, and [*smo-/-; SNAP-Smo; Ptch1-YFP]* cells, generated by introducing Ptch1-YFP into [*smo-/-; SNAP-Smo* cells]. For all constructs, after antibiotic selection, individual cell clones were isolated and tested for functionality of constructs, expression levels and responsiveness to SHH.

SNAP-Tag Labeling. Cells were labeled with 1 μM SNAP-Surface Alexa Fluor 647 (NEB) for 10–15 min at 37 °C, followed by three washes with 0.5% FCS tissue culture media.

ACP-Tag Labeling. The ACP-tag is a 77 AA protein tag based on acyl carrier protein from *E. Coli*, that can be enzymatically modified by using substrates that are derivatives of CoA (7). Cells were labeled with ACP-substrates according to manufacturer's recommendations (NEB). Briefly, cells were incubated with a freshly prepared staining mix containing 1 μM ACP-synthase, 1 μM CoA-DY647 substrate, and 10 mM Magnesium Chloride (all from NEB) in 0.5% FCS tissue culture media, for 30 min, at 37 °C, followed by three washes with fresh tissue culture media. For staining of fixed cells, just before fixation, cells were stained for 60 min with 5 μM CoA-biotin, fixed and subsequently stained with fluorescently tagged streptavidin.

Cholesterol depletion. Methyl-β-cyclodextrin (MβCD, Sigma) was dissolved in 0.5% FCS media. Cells were treated with 2 or 10 mM MβCD for up to 4h, as indicated for each experiment in the Results section.

Immunoblot Analysis. Cells were harvested into ice-cold PBS, lysed in RIPA buffer containing Protease Inhibitor Mixture (Roche) for 1 h at 4ºC. Samples were analyzed by standard immunoblot analysis and visualization using LI-COR Odyssey scanner.

Immunofluorescence, bulk microscopy and image analysis. Immunofluorescence and bulk microscopy were performed as previously described (5). Briefly, cells were fixed in ice-cold 4% (wt/vol) paraformaldehyde in phosphate buffered saline (PBS) for 10–15 min, permeabilized in a blocking solution containing 0.1% Triton X-100 and 1% normal donkey serum in PBS for 30 min. Cells were stained with primary and secondary antibodies diluted in the blocking solution for 1 hour each. All microscopy of fixed, immunostained cells was performed on a Leica DMIRE2 laser scanning confocal microscope. Images were taken with a 1.4 NA, 63x oil-immersion objective (Leica). Image analysis of protein levels in cilia was done in ImageJ (FIJI) as previously described. All quantitative comparisons for confocal image data were done using unpaired t-test (Prism 7 software). Data are presented as mean +/- SEM, and statistical significance in the figures is denoted as follows: NS- $p>0.05$, * $p<0.05$, ** $p<0.01$, *** $p<0.001$.

Cholesterol Visualization and Quantification Using EGFP-D4H Cholesterol Probe. In order to be able to detect cholesterol in cilia, we used SNAP-Smo cells treated with SAG. Cilia were identified using a fluorescent SNAP-substrate or an anti-SNAP antibody without any cell permeabilization. Cells were fixed and stained with EGFP-D4H and anti-SNAP diluted in PBS, at 4^{o} C, overnight. After several washes in PBS, cells were subsequently stained with a secondary antibody (to detect anti-SNAP), for 1 h at room temperature.

Quantitative Real-Time PCR. The mRNA levels of *gli1,* a direct Hh-target gene, were used as a metric for Hh pathway activation. Total cell RNA samples were isolated using TRIzol reagent (Invitrogen), and reverse-transcribed using SuperScript III First Strand Kit (Invitrogen). The transcript levels for *gli1* were quantified by real-time PCR (Applied Biosystems 7500) using TaqMan gene expression probes (Applied Biosystems) for gli1 (Mm00494645_m1) and gapdh (Mm99999915_g1) to normalize the samples. Real-time PCR data were analyzed by unpaired t test (Prism 7 software), and presented as mean +/- SEM. Statistical significance in the figures is denoted as follows: NS- $p>0.05$, * $p<0.05$, **$p<0.01$, ***$p<0.001$.

B. Single-Molecule Imaging and Analysis

Single-molecule imaging set-up. Single-molecule imaging experiments were performed using an inverted microscope body (IX71, Olympus), outfitted with a motorized stage (M26821LOJ, Physik Instrumente) controlled via customized MATLAB scripts and a stage-top incubator at 37° C (INUB-PI-F1, Tokai Hit, Japan). PTCH1 proteins, labeled with the ACP substrate CoA-DY647 (a derivative of the Dyomics dye DY-647P1) and SMO proteins, labeled with SNAP-Surface Alexa647 (both from NEB) were illuminated at moderate intensities (~700 W/cm^2) using circularly polarized light from a 638 nm laser (FiberTec II, Blue Sky Research). Yellow fluorescent protein (YFP) molecules labeling the C-terminus of the PTCH1 were excited by circularly polarized light from a 514 nm laser (Sapphire, Coherent) at low intensities to track cilia (~100 W/cm^2), and at high intensities for simultaneous super-localization experiments (~1-5 kW/cm^2). Both illumination lasers were modulated using two acousto-optic modulators (AOM, 1205C-2, Isomet) in alternating 16 ms exposures centered during 20 ms camera frames. Cameras and lasers were synced using a Digital Delay Generator (DG645 Stanford Research Systems). Fluorescence was collected through a 1.4 NA, 100x, oil-immersion objective (UPLSAPO, Olympus) and passed through a dichroic filter (FF425/532/656-Di01 Semrock). Longer wavelength light from the Alexa647 or DY647 fluorophores was passed through a long pass dichroic (FF580-Di01, Semrock) and a band pass filter (680-60, Chroma) before being imaged on a Si EMCCD camera (iXon897 Ultra, Andor). Fluorescence from YFP was reflected by the second dichroic, filtered by a bandpass filter (545-40, Semrock) and then imaged on a second Si EMCCD camera, as diagramed in **Fig. S2** (iXon897 Ultra, Andor).

At the beginning of each experiment, cell media was replaced with imaging media containing the oxygen scavenger pyranose oxidase and catalase (both from Sigma). The slide was then explored at low-illumination intensity (~10 W/cm^2) for ~10 minutes while recording the coordinates of cilia, which were marked by PTCH1-YFP or elevated concentrations of SMO (in accumulation conditions). After 10-20 cilia were identified, fluorescent molecules in each cilium were imaged for several minutes as described, so that no cell-sample was imaged for more than 1.5 hours. We have previously shown that this treatment did not abrogate the signaling pathway (5).

Two-Color Image Registration. Images recorded on the two cameras were aligned using sparse fluorescent bead (F8792, Invitrogen) samples in poly-vinyl alcohol (PVA, Sigma) visible in both channels that were scanned across the field of view in a grid pattern using a precision x-y piezo stage (**Fig. S3**). Beads were localized in each frame and channel using a 2D symmetric Gaussian function, and then used to calculate an affine transformation function using Matlab. Image analysis (tracking & localizations) was performed on raw data before the transformation function was applied in order to avoid pixilation artifacts.

Single-Molecule Tracking. Trajectories were recorded and analyzed using custom scripts written in MATLAB. In each frame, single-molecule emitters were localized by fitting a 2D symmetric Gaussian function (which well-approximates the point spread function of the microscope) with a constant offset using the non-linear least squares fit algorithm *lsqnonlin*. Localizations with unphysical parameters were removed, likely being caused by rare fluctuations in the background or nearby molecules. Because of the wide separation between molecules, and the typical diffusive motion with diffusion coefficient ~0.2 $\mu m^2/s$, localizations in sequential frames could be readily identified as the same molecule. In ambiguous cases where two molecules moved close together, trajectories were ended, and begun as new trajectories after the molecules were once again well separated. Single-molecule blinking was permitted within a trajectory in cases meeting three criteria: (1) the molecule blinked on again in fewer than 200 ms (5 frames), (2) no other fluorescent molecules were nearby, and (3) there was fairly small spatial displacement during the blinked-off period. If one of the above criteria was not met, tracking continued as a separate molecule. In most cases, trajectories ended abruptly, caused by photobleaching events of the individual fluorophore. In rare cases, multiple signal brightness levels were observed during otherwise apparent single-molecule trajectories, indicative of the presence of multimers. Only trajectories with a single brightness level were used for further analysis of single-molecule motion.

Trajectory Analysis. The goal of our analysis algorithm is to classify the various periods of motion within a trajectory as either confined (remaining static within the precision of the measurement), directed (traveling with a continuous and stable velocity), or diffusive (motion characterized by Brownian diffusion). Classification within the primary cilium is

confounded by the small dimensions of the organelle and the spatial error associated with localization. Our approach is therefore to find a ciliary axis, measure the axial and lateral movement separately, and then determine the motion type while weighting the axial movement more heavily.

The ciliary axis is found by taking diffraction-limited images of the cilium, and identifying the approximate long and short axes manually. A spline is then calculated by fitting a smooth curve through the cilium using even spaced (160 nm) 1D Gaussian fits across the selected region. We accommodated for slightly curved cilia by adding additional points to the spline fit. The base and tip are then defined manually, and each localization is redefined in axial and lateral coordinates. This is done by finding the closest point along the spline and integrating the total curve length from the base as the axial position and the distance between the localized position and the closest axial point as the lateral distance. The normalized axial position is defined as the ratio of the curve length from the base to the axial position to the curve length from the base to the tip; it is only used to aggregate results in different cilia.

Trajectory analysis then begins by examining short, overlapping subtrajectories consisting of 11 frames. From these short periods, three parameters are estimated which correspond to the relative probability of that subtrajectory being bound, diffusive, or moving linearly by comparing the consistency of the positions and displacements to expected distributions for these movement types. Distributions of displacements are described by the normal distribution (Equation 1), where $P\left(\Delta x(t)\right)$ is the probability of moving $\Delta x(t)$ in time t.

$$P\left(\Delta x(t)\right) = \frac{1}{\sqrt{2\pi s^2}} \exp\left(-\frac{\left(\Delta x(t) - \mu\right)^2}{2s^2} \right) \tag{1}$$

The mean displacement, μ, is equal to zero for bound or diffusive motion and equal to the product of $velocity \times time$ for directed transport. The standard deviation of the distribution, s, is equal to $\sqrt{2 \cdot \sigma_{loc.prec.}}$ for statically bound and directed subtrajectories, and $\sqrt{2Dt + 2\sigma_{loc.prec.}{}^2)}$ for diffusive subtrajectories where D is the expected diffusion

coefficient, t is the product of the *timelag* and *framelength*; $\sigma_{loc.prec.}$ is the static localization precision.

The resulting three parameters for each timestep are next passed through a built-in denoising wavelet filter in Matlab, *wden*, to reduce the fluctuations, but preserve the overall structure. Frames that were classified as linear motion, but with either very high (>4 μm/s) or very low linear velocities (<100 nm/s) were reevaluated to determine if they were likely diffusive or bound, respectively.

We are primarily interested in dividing a trajectory into subtrajectories of various types of motion, not so much the likelihood of an individual frame being a specific motion type. Adjacent frames were grouped by their initial classification; anterograde and retrograde periods are distinguished based on their movement direction, and the boundaries between these classifications were adjusted by checking for consistency with the neighboring motion types. This process is done multiple times, where each repeat consists of a diffusion, binding, & directed motion evaluation step followed by a recombination step.

The parameters used in this process were optimized by using trajectory simulations in cylindrical objects to quantitate the relative errors in classification, and by reviewing the output on real data and ensuring rough agreement with manual classification. The end result is that a subtrajectory is classified as confined if it remains within a position for > 0.2 s; directed if it moves in one direction continuously within the limits of the localization precision of each step; diffusive if the measured displacements between frames in a short subtrajectory are consistent with the expected distribution for a membrane-protein; and unclassified when any of the previous descriptions do not apply, most frequently when several frames between two determined subtrajectories are statistically inconsistent with their neighbors. While the classification algorithm does not achieve perfect identification of the underlying movement type, we found that the general trends observed in our data were robust to a broad range of parameters and the addition/deletion of various steps in our algorithmic approach. Simulation and analysis code available upon reasonable request.

Diffusion coefficient analysis. To quantify the diffusion coefficients for PTCH1 and SMO, identified diffusive subtrajectories containing 25 or more frames were first divided into equal-length 25-frame segments. Per segment, a linear fit to the mean squared displacement (MSD) curve using the first and second time lags was calculated for motion along the long axis of the cilium, where the slope is proportional to the diffusion coefficient, and the offset is due to a combination of motion blur and measurement precision.

Directed-velocity measurements. The average anterograde and retrograde velocity were calculated from identified directed subtrajectories. To validate these measurements, we compared the results to traditional kymogram measurements made on clusters of molecules seen in the cilium (**SI Video 5**). Kymogram velocities were calculated by analyzing the slope of apparent linear motion along the axial position over time (**Fig. S4**).

Classification analysis by trajectory simulation. To evaluate the propensity of our analysis to misclassify subtrajectories, we simulated three types of motion in cilia-like structures and analyzed the results (**Fig. S6**).

Error estimation of single-molecule results by bootstrapping. To calculate the significance of each single-molecule-based conclusion for PTCH1, we estimated the measurement error by quantifying the contribution of each trajectory to the overall result. This was done by resampling random sets of the single-molecule trajectories and calculating the variance (i.e. bootstrapping with the same number of total trajectories). For SMO, where trajectories were longer on average, we performed a similar analysis, but resampled portions of trajectories such that the total duration of measured data was equally analyzed. Trajectories shorter than 1 second were removed. We repeated this process 1000 times and compared the results between conditions (i.e. bootstrapping with the same total trajectory durations).

References

1. Bishop B, *et al* (2009) Structural insights into hedgehog ligand sequestration by the human hedgehog-interacting protein HHIP. *Nat Struct Mol Biol* 16(7): 698-703.

2. Maekawa M & Fairn GD (2015) Complementary probes reveal that phosphatidylserine is required for the proper transbilayer distribution of cholesterol. *J Cell Sci* 128(7): 1422.

3. Rohatgi R, Milenkovic L & Scott MP (2007) Patched1 regulates hedgehog signaling at the primary cilium. *Science* 317(5836): 372-376.

4. Phua SC, *et al* (2017) Dynamic remodeling of membrane composition drives cell cycle through primary cilia excision. *Cell* 168(1): 264-279.

5. Milenkovic L, *et al* (2015) Single-molecule imaging of hedgehog pathway protein smoothened in primary cilia reveals binding events regulated by Patched1. *Proc Natl Acad Sci U S A* 112(27): 8320-8325.

6. Milenkovic L, Scott MP & Rohatgi R (2009) Lateral transport of smoothened from the plasma membrane to the membrane of the cilium. *J Cell Biol* 187(3): 365-374.

7. George N, Pick H, Vogel H, Johnsson N & Johnsson K (2004) Specific labeling of cell surface proteins with chemically diverse compounds. *J Am Chem Soc* 126: 8896-8897.

C. Supplementary Figures

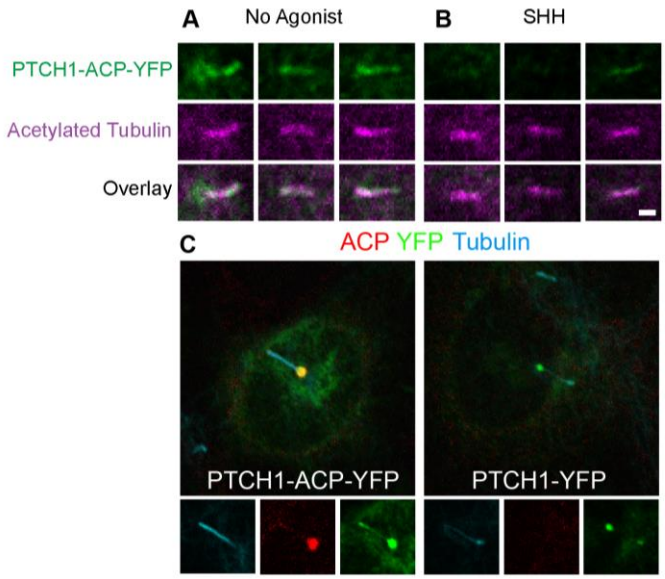

Fig. S1: PTCH1-ACP-YFP accumulates in cilia (**A**), and delocalizes after SHH treatment (**B**). Cells were fixed, stained with anti-YFP and anti-Acetylated Tubulin antibodies and imaged with standard confocal microscopy. Three representative cilia are shown per group. Scale bar is 1 µm. **C)** Labeling with the ACP substrate is specific. PTCH1-ACP-YFP protein is readily labeled with non-cell-permeable ACP-substrate in diffraction-limited imaging. NIH3T3 cells were transiently transfected with PTCH1-ACP-YFP (left) or PTCH1-YFP (right) and stained with biotin-ACP substrate. The staining is specific: only cells expressing PTCH1-ACP-YFP show staining with the ACP substrate.

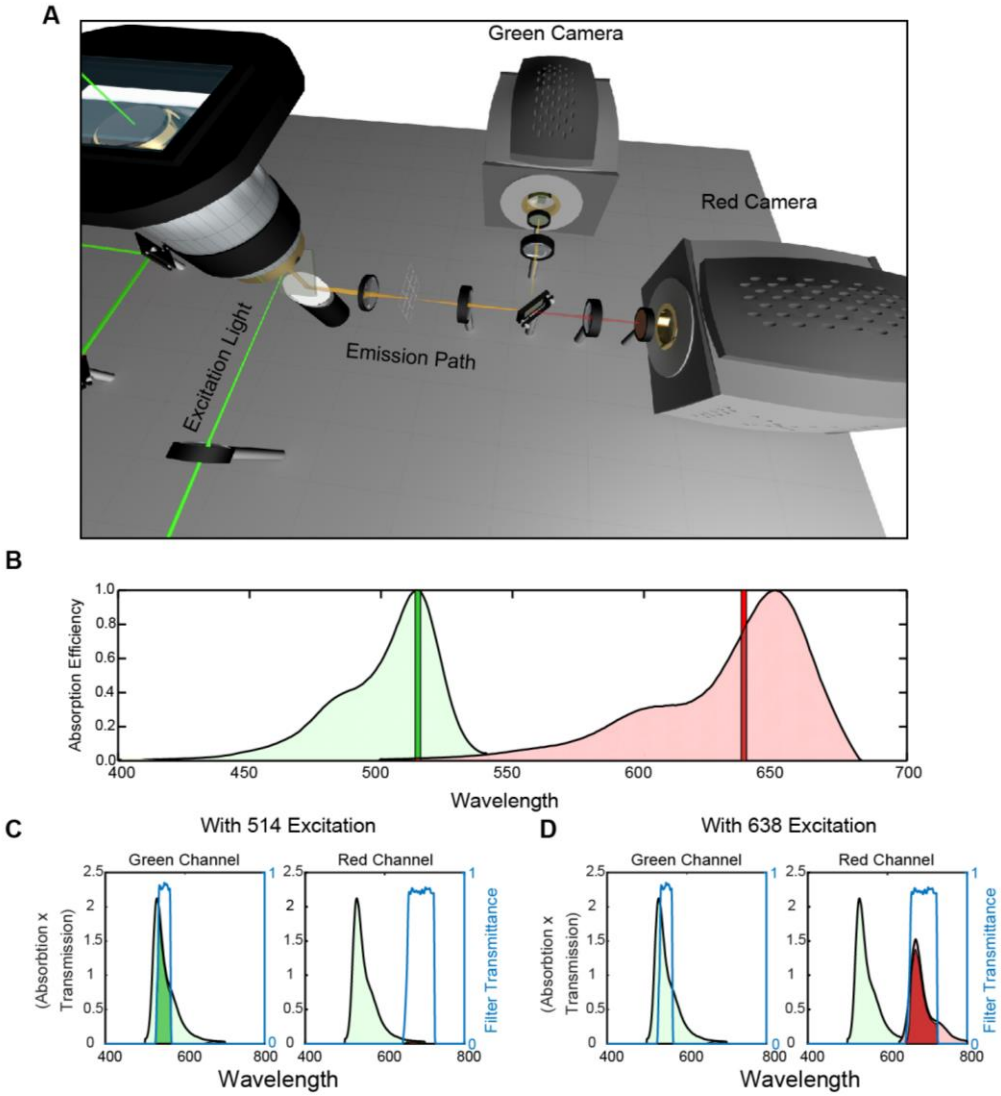

Fig. S2: Emission path of the single-molecule microscope. **A)** 3-D Illustration of the emission path. Light collected through the microscope objective is chromatically separated from the excitation light using a dichroic mirror. The remaining light is then split into red and green channels by a second dichroic mirror. Finally, each channel is chromatically filtered before being detected by two cameras. **B)** The absorption spectra of YFP (green), and Alexa647 (red). DY647 emission is similar. The bright vertical bands represent the pumping light. **C)** When excited with a 514 nm laser, the resulting spectra that are observed in each channel after chromatic filtering are highlighted. **D)** Same as (C), but after 638 nm excitation.

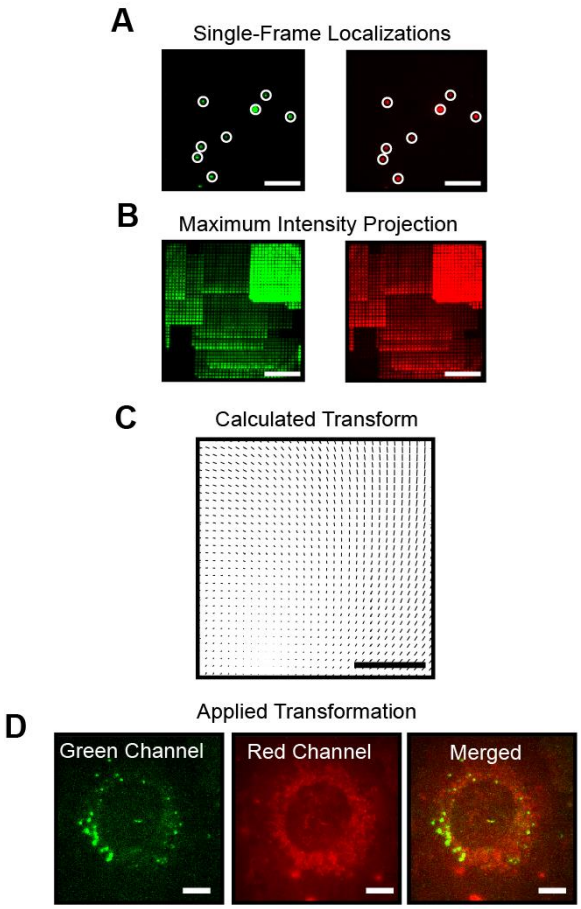

Fig. S3: Multicolor-Image Alignment. **A)** Groups of fluorescent beads with broad emission are imaged in both channels and localized. **B)** The sample is scanned to obtain a dense field of positions measured in both imaging channels. **C)** The reference points are used to calculate an affine transform. **D)** Green and red positions and images can be precisely overlaid.

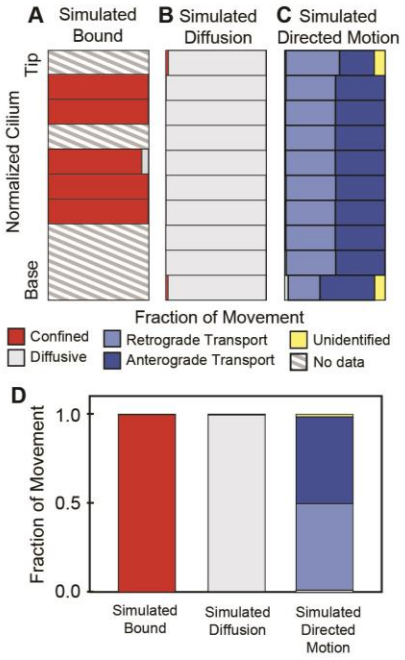

Fig. S4: Analysis of simulated trajectories. (**A-C**) three types of motion were simulated in cilia-like structures and analyzed using the same classification algorithm used to analyze our single-molecule trajectories in Figs. 3 & 4. (**D**) The aggregated data integrated over the entire length of the structure.

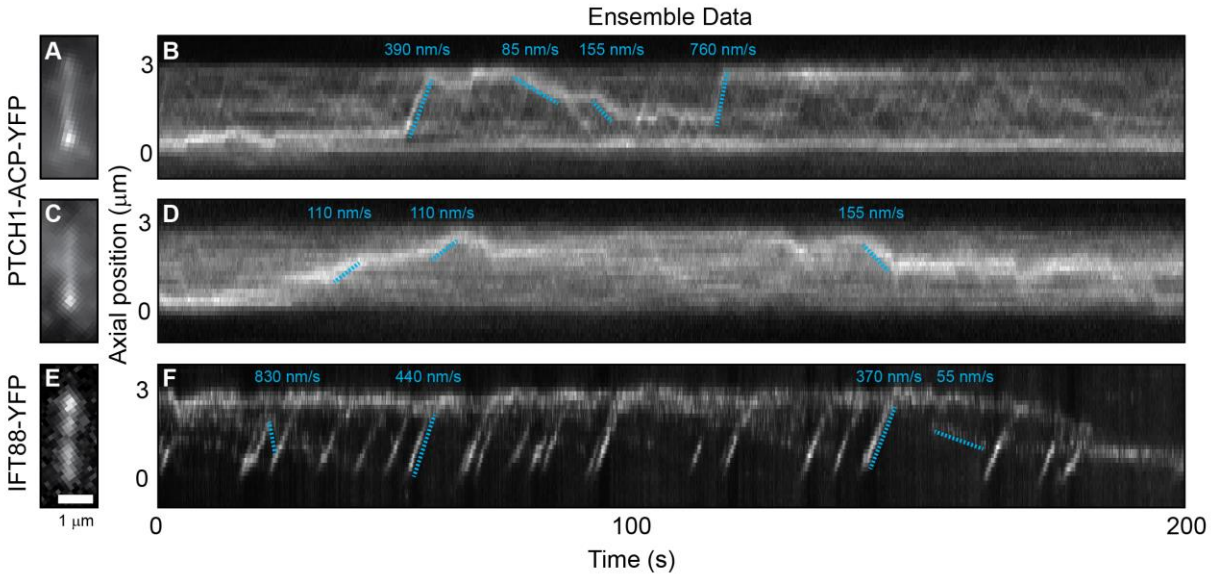

Fig. S5: Kymogram velocity measurements in cilia. (**A-D**) PTCH1-ACP-YFP clusters visualized in the YFP channel. (**E,F**) IFT88-YFP recorded in IMCD3 cells. Left images show the 2D cilium. Right images show the intensity projections along the ciliary axis over time. Velocities for selected periods of apparent directed motion are highlighted in blue.

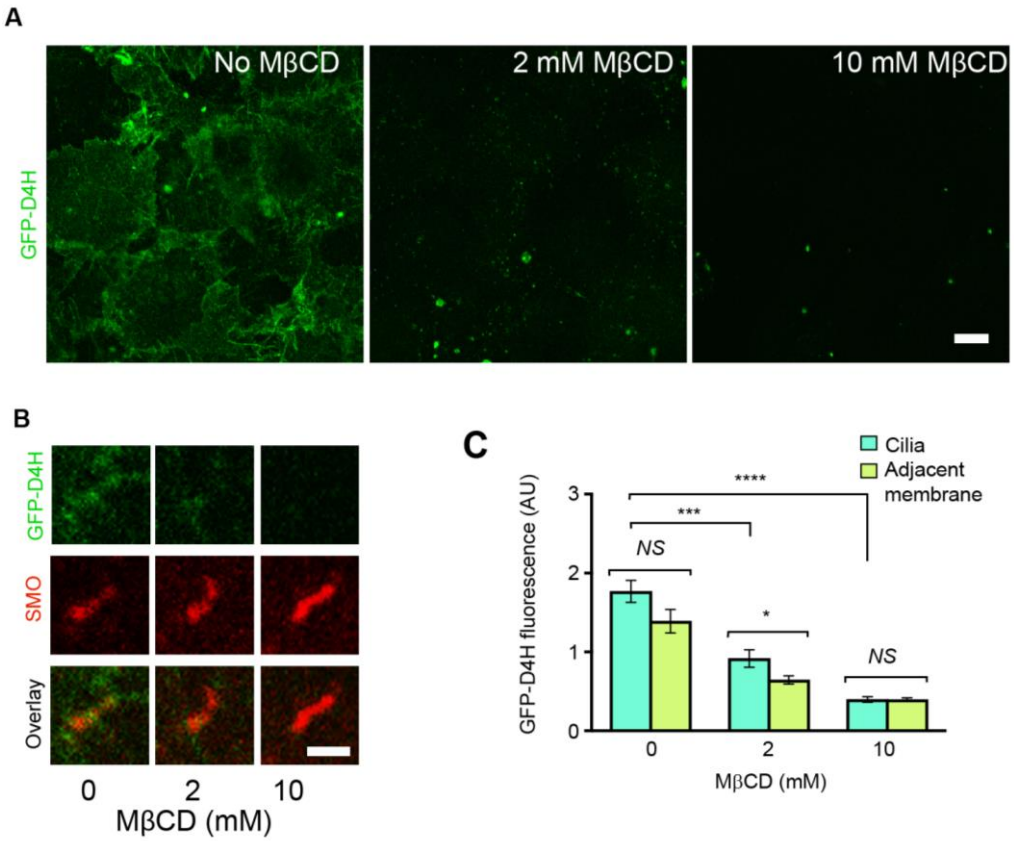

Fig. S6: Treatment with MβCD decreases the levels of cholesterol in cilia and in the adjacent plasma membrane in diffraction-limited imaging. **A)** Cells stained with EGFP-D4H cholesterol-binding probe. For cholesterol depletion, cells were treated with MβCD for 30 min and subsequently fixed. Scale bar; 10µm. **B)** EGFP-D4H staining in cilia. Cells were pre-treated with SAG for 24h to induce SNAP-SMO in cilia, and the presence of SNAP-SMO was extracted by immunofluorescence. Scale bar: 2µm. **C)** EGFP-D4H staining was quantified for ciliary and adjacent plasma membranes (equal area). Graph shows mean +/- SEM (NS- $p>0.05$; * $p<0.05$; *** $p<0.001$). Treatment with MβCD decreases the levels of cholesterol in cilia and the adjacent plasma membrane.

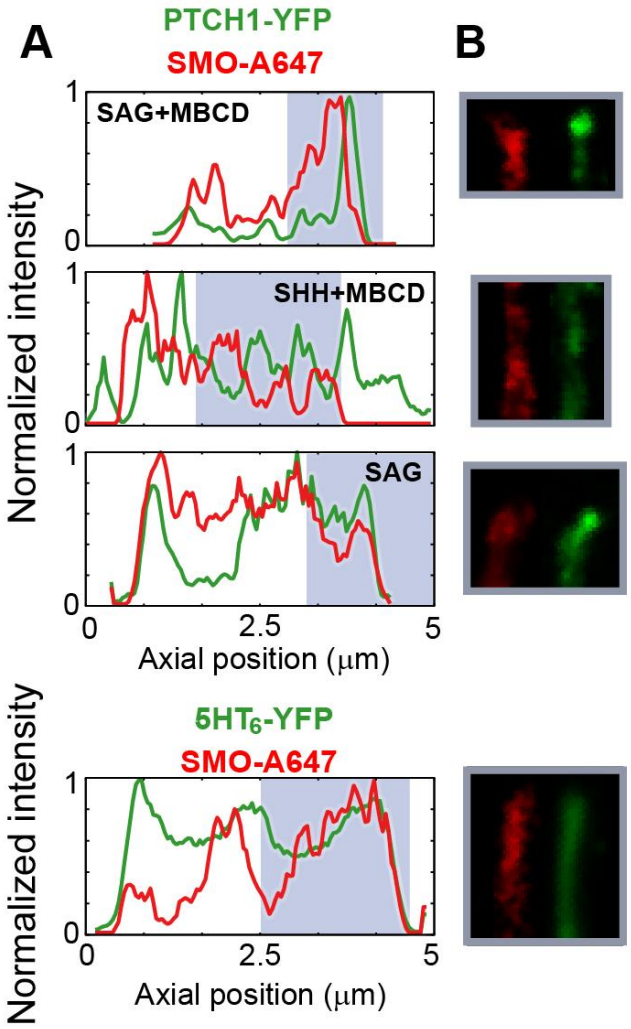

Fig. S7: Normalized distribution of localizations measured in primary cilia. The super-localized data used to create the 2D histograms in Figure 5 were replotted as line profiles along the axial extent of the cilia. Data was integrated over the lateral position. Localizations from trajectories of SMO molecules are plotted in red, while the localizations of **A**) PTCH1-YFP and 5HT6-YFP are shown in green. **B**) 2D histograms of each color channel in the regions highlighted in **A**, where the height of the image corresponds to the width of the highlighted area.

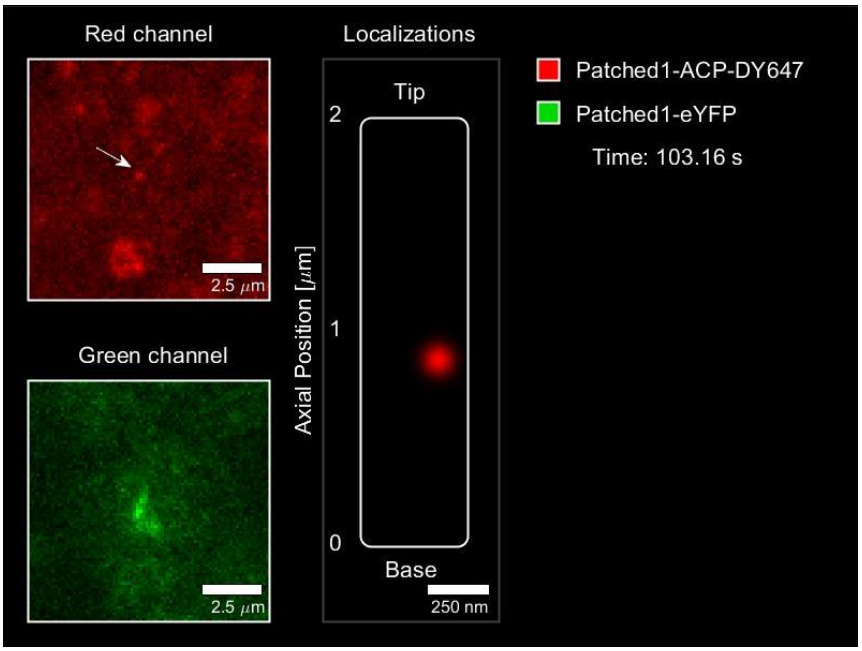

Video S1: Simultaneous recording of two color channels, DY647 and YFP, for single, double-labeled PTCH1-ACP-YFP molecules. (Top left) Camera data recorded in the red channel. (Bottom left) Camera data recorded in the green channel. For clarity, each frame is shown as a 160 ms integration of 40 ms frames. (Right): Localized and aligned position of a PTCH1-ACP-YFP molecule, relative to the cilium.

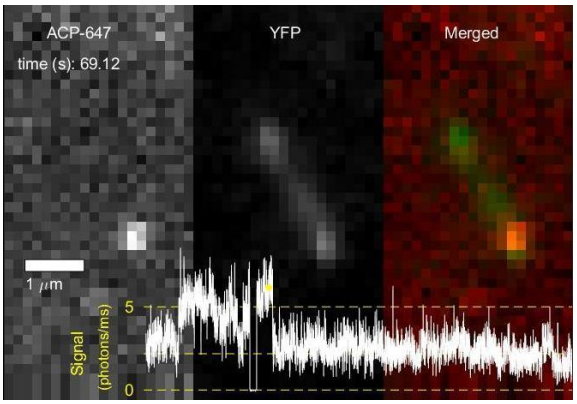

Video S2: Multiple, discrete photon-levels observed for DY647 labeled PTCH1-ACP-YFP. (Left) Camera data recorded in the red channel. (Middle) Camera data recorded in the green channel. (Right): The overlay of recorded red and green data showing the positions of individual PTCH1 proteins and ensemble distribution. For clarity, movies are shown as 320 ms integrations of 40 ms frames. The lower plot shows the mean signal photons per ms during each 320 ms bin.

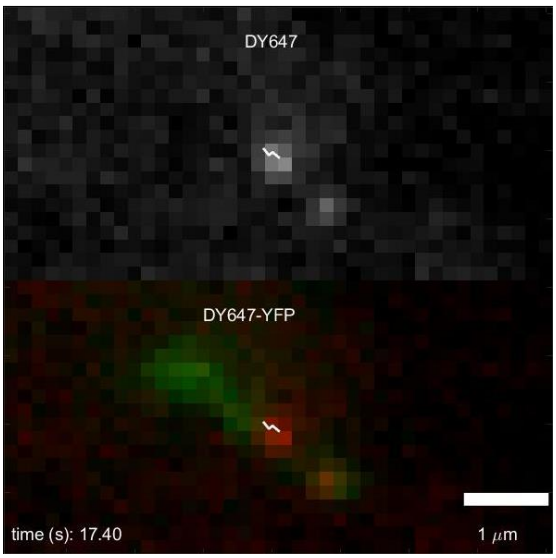

Video S3: Directed motion observed for DY647 labeled PTCH1-ACP-YFP. (Top) Camera data recorded in the red channel, overlaid with the tracked position. (Bottom): The same data as above, but overlaid with a single image of single image of the ensemble distribution of PTCH1-ACP-YFP recorded before the trajectory. For clarity, each frame is shown as a 160 ms integration of 40 ms frames.

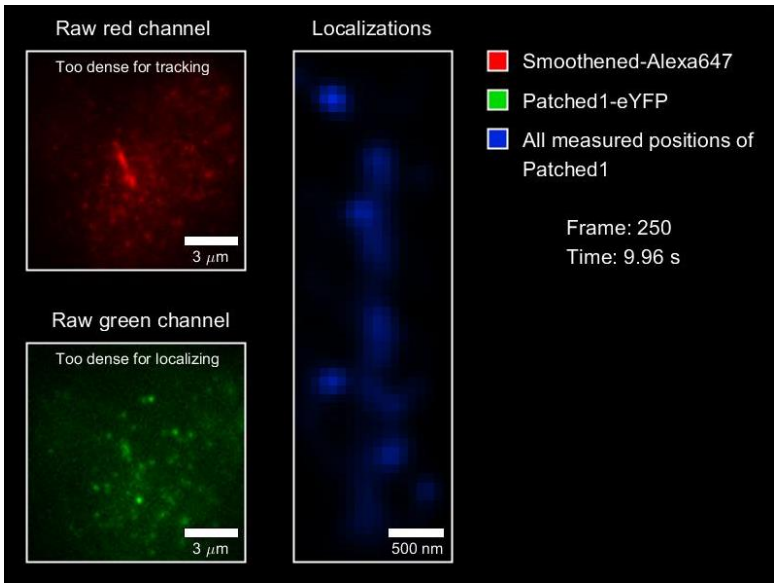

Video S4: Simultaneous SMO-A647 tracking with super-localized PTCH1-YFP molecules. (Top left) Camera data recorded in the red channel. (Bottom left) Camera data recorded in the green channel. (Right): Localized and aligned data from both channels plotted simultaneously, SMO-A647 trajectories plotted in red, PTCH1-YFP localizations plotted in green, and the aggregated localizations of PTCH1-YFP plotted in blue. Note that SMO molecules are only tracked when the concentration is sufficiently low to have no overlapping molecules.

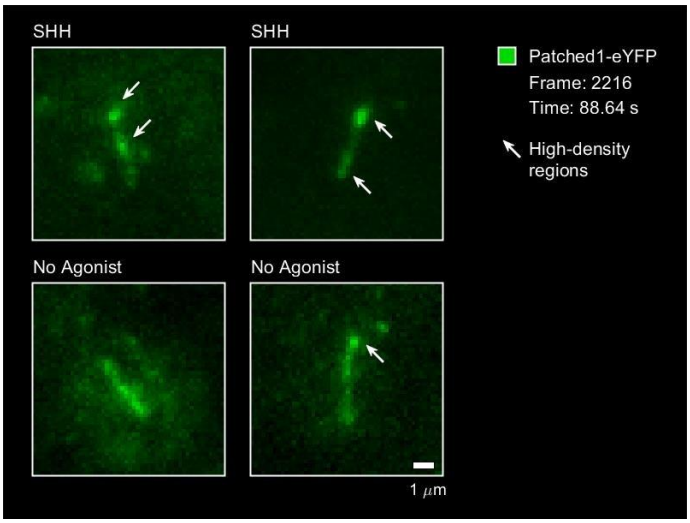

Video S5: Ensemble data of PTCH1-ACP-YFP in the cilium. Clusters of PTCH1 molecules are dynamically observed in cilia, often moving together (white arrows).